

*Electronic supplementary information for*

Why is tris(trimethylsilyl) phosphite effective as an additive  
for high-voltage lithium-ion batteries?†

*Young-Kyu Han\* and Jaeik Yoo*

Department of Energy and Materials Engineering and Advanced Energy and Electronic  
Materials Research Center, Dongguk University-Seoul, Seoul 100-715, Republic of Korea

*Taeun Yim\**

Advanced Batteries Research Center, Korea Electronics Technology Institute, Seongnam,  
Gyeonggi 463-816, Republic of Korea

\* E-mail: [ykenery@dongguk.edu](mailto:ykenery@dongguk.edu) and [yte0102@keti.re.kr](mailto:yte0102@keti.re.kr)

**Fig. S1 (a) Molecular structures of tris(trimethylsilyl) phosphite (TMSP)**

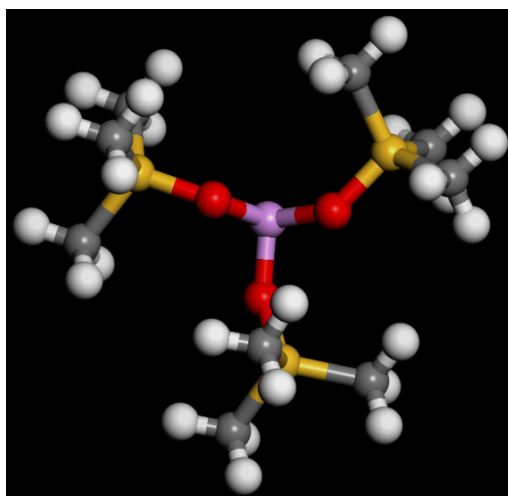
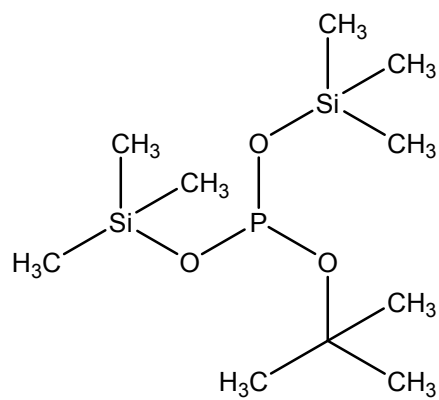


**Fig. S1 (b) Molecular structures of tris(trimethylsilyl) phosphate**

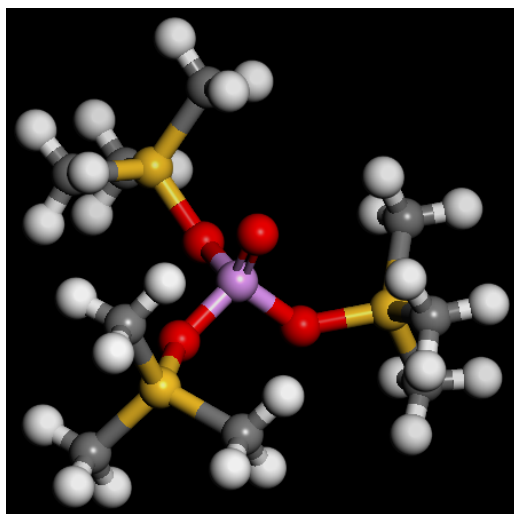
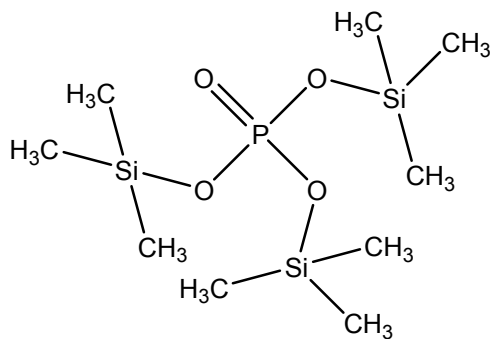


**Fig. S1 (c) Molecular structures of tris(trimethylsilyl) borate (TMSB)**

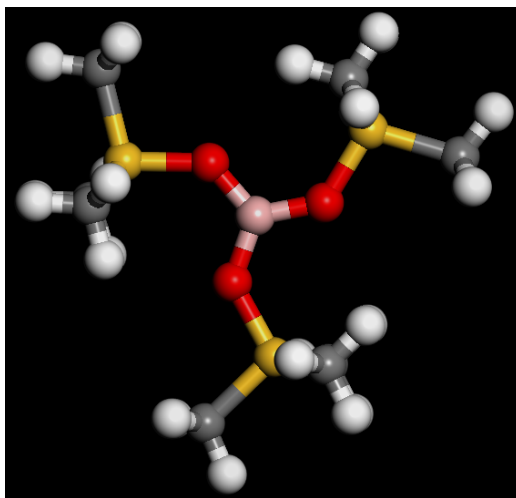
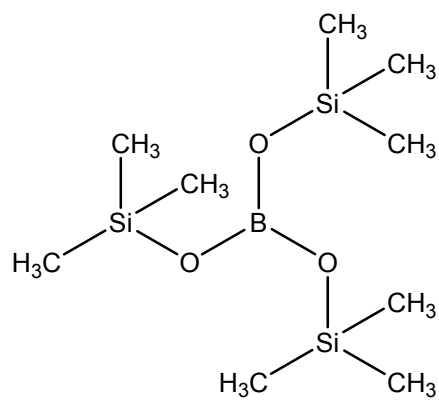


**Fig. S2 (a) Correlation between HOMO and oxidation potentials**

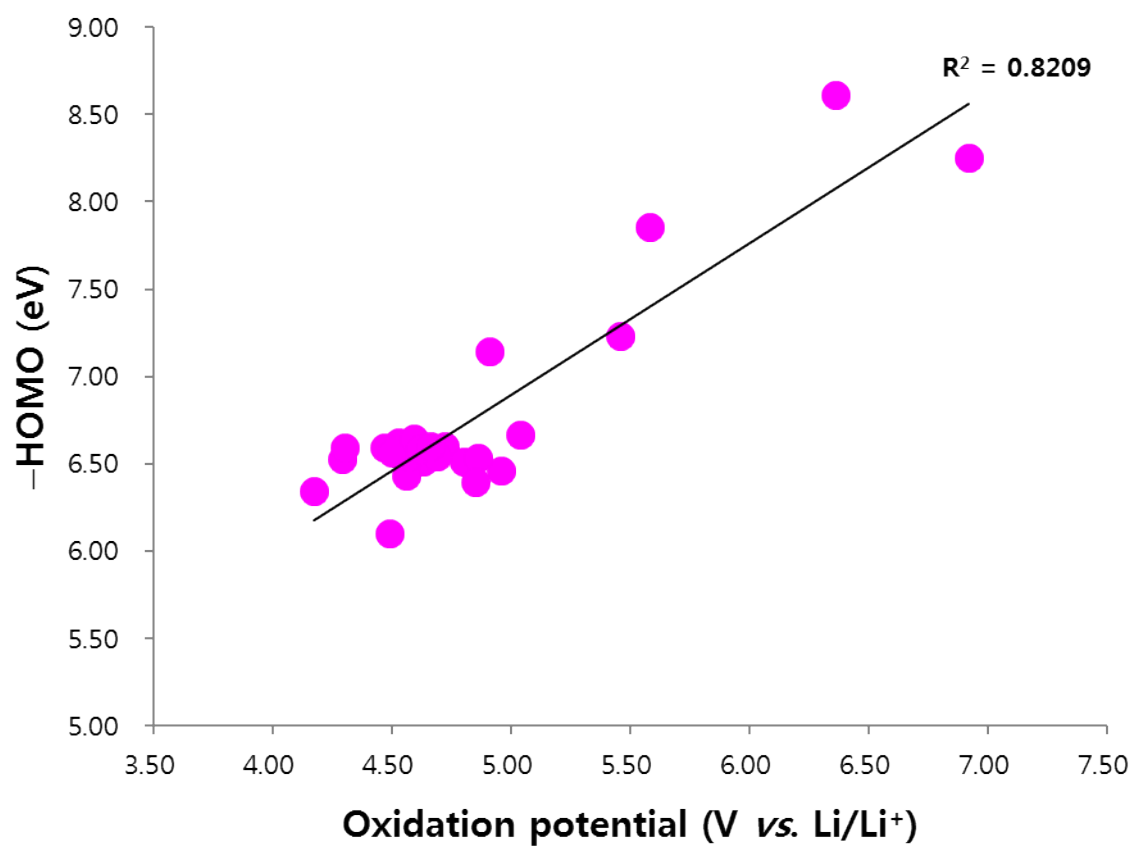


Fig. S2 (b) Correlation between LUMO and reduction potentials

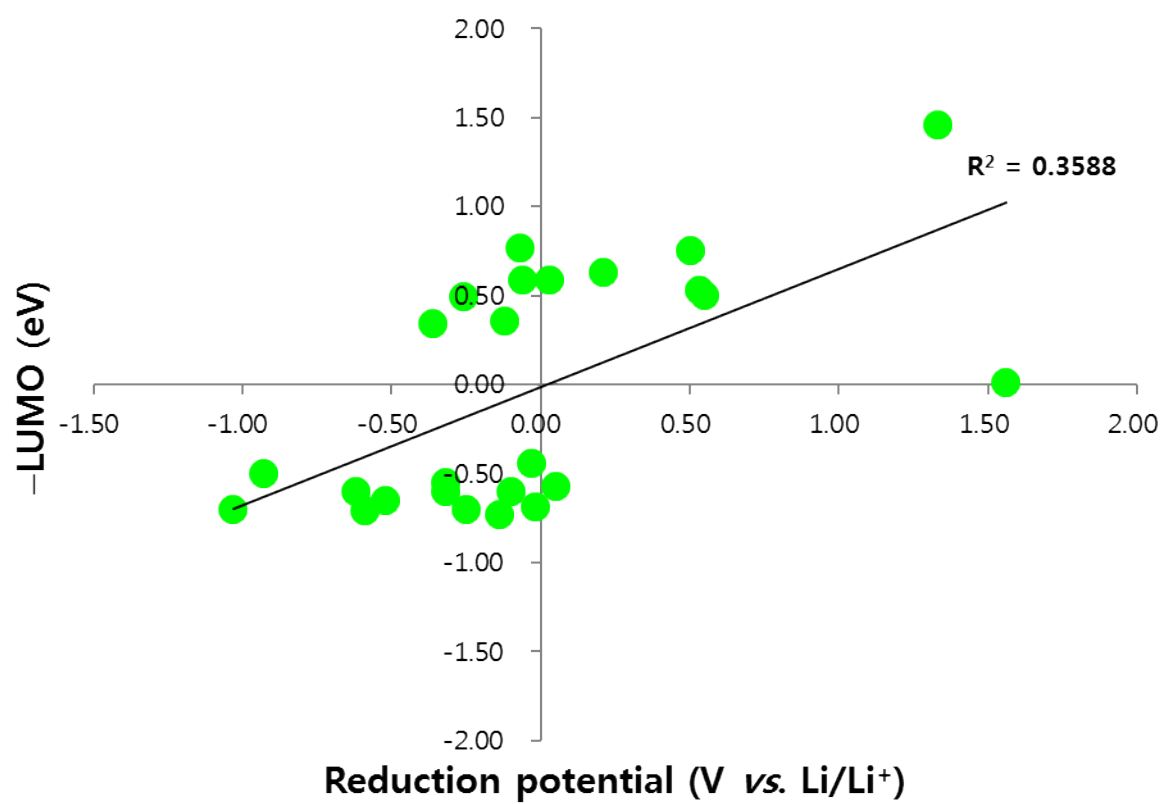
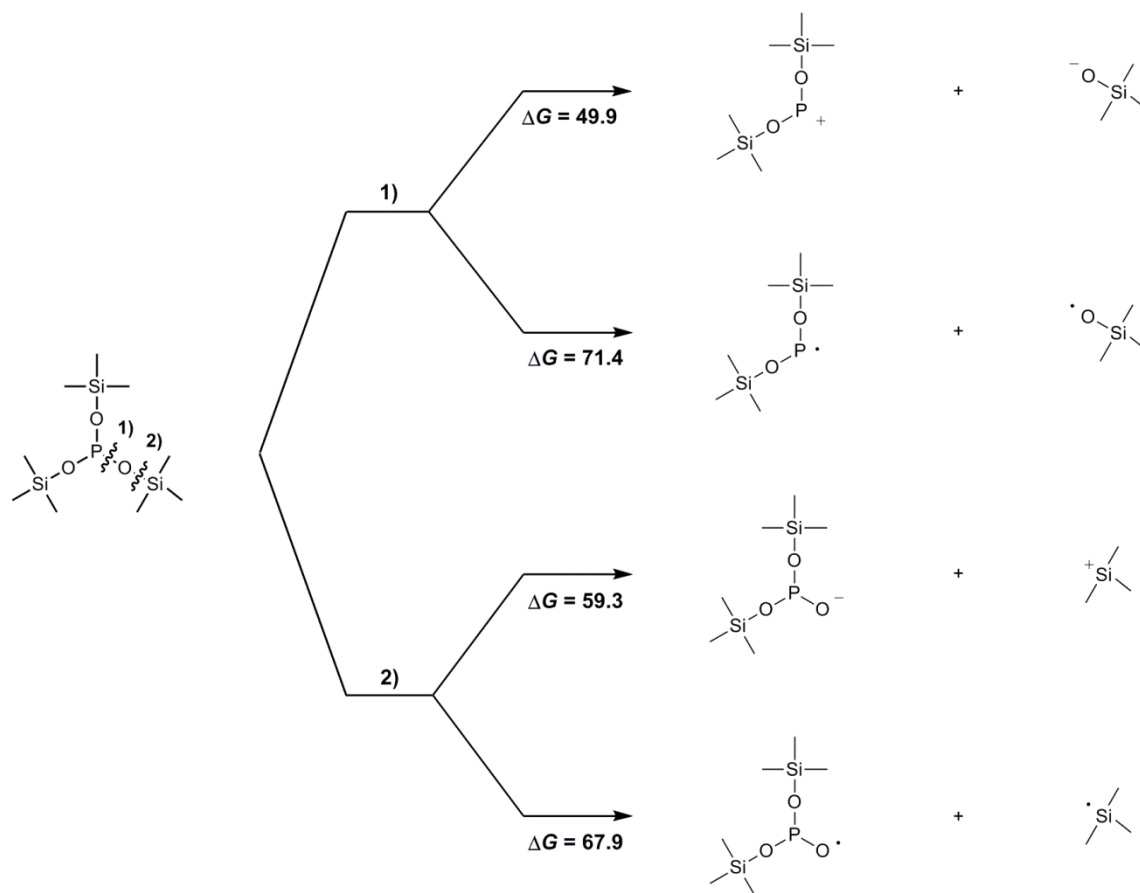


Fig. S3 Decomposition reaction energies of neutral TMSP (Units are in kcal/mol)



## Synergetic effects of TMSP and VC

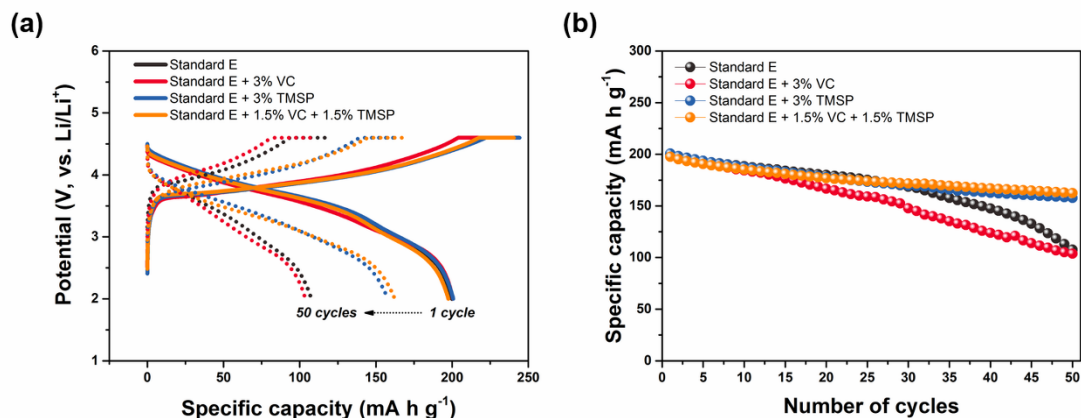


Fig. S4. (a) Potential profiles of the half cells, and (b) their cycling performance with (i) no additive (black), (ii) 3% VC (red), (iii) 3% TMSP (blue), and (iv) 1.5% VC + 1.5% TMSP (orange)

To investigate the synergetic effects of TMSP and VC, we performed a half-cell experiment for each cell composed of different electrolyte compositions depending on the additives. The potential profiles and cycling performances are presented in Fig. S4. The cell cycled with VC exhibited a significant fading of cycle life (51.7% of retention at 50 cycles), even compared to the cell cycled with a standard electrolyte (53.8% at 50 cycles). On the contrary, the cell controlled with TMSP indicated significant improvement in cycling performance in which about 80% of the specific capacity still remained at the ends of the cycles in the cells cycled with 3% TMSP (blue) and 1.5% TMSP + 1.5% VC (orange). This implies that the electrochemical oxidation of TMSP creates a stable passivation layer on the OLO surface, which is responsible for mitigating undesirable electrochemical decompositions of VC.



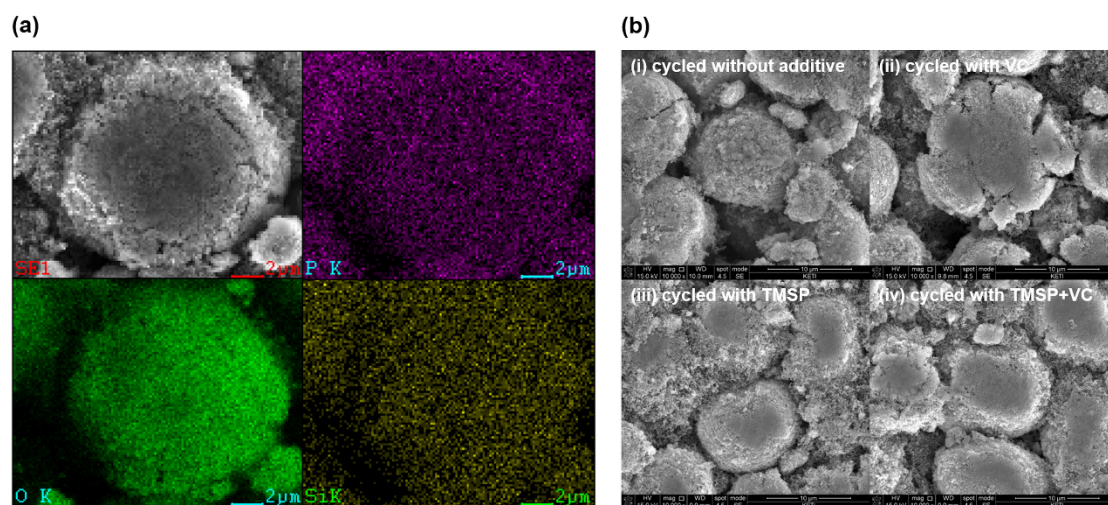


Fig. S5. (a) SEM-EDS result for OLO electrodes cycled with 1.5% VC and 1.5% TMSP, (b) SEM analyses for cycled OLO electrodes: (i) pristine, (ii) with 3% VC, (iii) with 3% TMSP, and (iv) with 1.5% VC and 1.5% TMSP

In order to probe the formation of the surface layer via the electrochemical reaction of TMSP, the cycled OLO electrode controlled with 1.5% VC and 1.5% TMSP was analyzed by SEM-EDS (energy dispersive spectroscopy), as shown in Fig. S5a. The cycled electrode showed the existence of relevant elements, such as carbon, phosphorous, oxygen, and silicone, which correspond to the chemical structure of TMSP. This indicates that TMSP (and/or oxidized  $\text{TMSP}^+$  species) appears to participate in the formation of a passivation layer on the OLO electrode, resulting in changes of the surface chemistry. The SEM analyses for cycled OLO electrodes support the electrochemical performance results (Fig. S5b). While the OLO electrodes cycled with a standard electrolyte and only VC appear to be severely degraded, the TMSP-controlled electrodes showed a relatively clean surface morphology along with less cracks at the ends of cycling. This indicates that TMSP forms an effective surface layer on the OLO electrode surface, which suppresses additional VC decomposition during the electrochemical process. Previous research papers support our experimental results in that the effective functional additive can be decomposed by electrochemical reactions during the initial formation step, and this allows for new coverages to be developed on the electrode surface, which is responsible for deactivating the electrochemically active sites.<sup>1-3</sup>

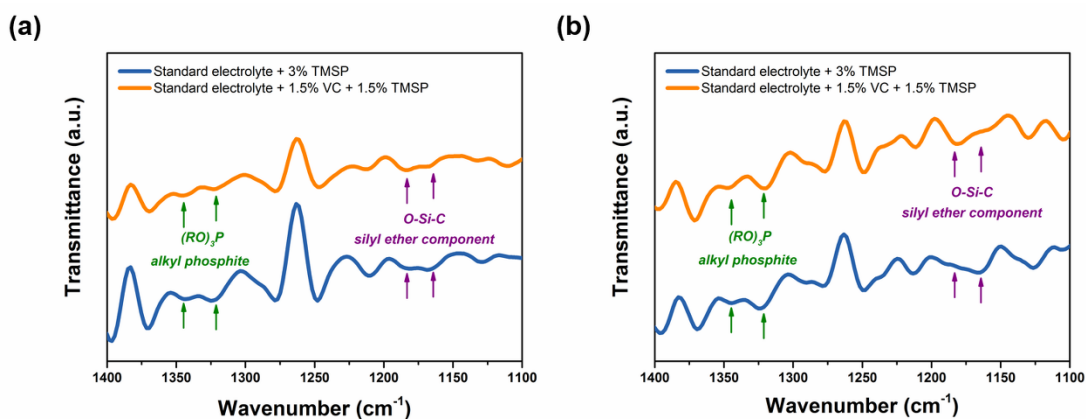


Fig. S6. FT-IR analyses for cycled electrodes after (a) 1 cycle and (b) 50 cycles (3% TMSP (blue) and 1.5% VC + 1.5% TMSP (orange))

To examine the chemical connectivity of the developed surface layer by the electrochemical reaction of TMSP, cycled electrodes controlled with TMSP were analyzed by FT-IR, as shown in Fig. S6. The TMSP-controlled electrodes revealed distinct transmittance signals that corresponded to the molecular structure of TMSP, and alkyl phosphite ((RO)<sub>3</sub>P, 1344 and 1321 cm<sup>-1</sup>) and silyl ether components (O–Si–C, 1184, and 1164 cm<sup>-1</sup>) were observed after the initial formation step.<sup>4</sup> The observed chemical connectivities are very similar to the chemical structure of TMSP, and therefore the TMSP appears to contribute to the formation of the surface layer as we proposed. Interestingly, each surface layer component showed a quite different spectroscopic behavior in which even when (RO)<sub>3</sub>P signals still remained at the ends of cycling, the transmittance signals that corresponded to the O–Si–C connectivity appeared to be faded compared to the initial cycle. This may imply a positive effect of TMSP associated with the HF scavenging reaction: the element “Si” has a high binding affinity with the HF species.<sup>5,6</sup> Therefore, the O–Si–C connectivity would scavenge the remaining HF in the electrolytes and contribute to suppressing (or mitigating) a dissolution of the transition metal components. Based on the spectroscopic evidence, we concluded that the TMSP would enhance the interfacial stability of the positive electrode by the formation of effective protection layers, and it may suppress continuous VC decomposition during electrochemical charging/discharging processes. This allows the cell to be more applicable, particularly for high-voltage operating electrodes.

### ***Experimental section***

To examine the electrochemical performance of TMSP, positive electrodes were prepared as follows. To prepare the cathode, a mixture of 0.5  $\text{Li}_2\text{MnO}_3 \cdot 0.5 \text{Li}(\text{Ni}_{0.4}\text{Co}_{0.2}\text{Mn}_{0.4})\text{O}_2$  (OLO, Ecopro), poly(vinylidene fluoride) (PVdF) (Kureha, KF1100), and Super P (carbon black) at a weight ratio of 92:4:4 was dispersed in *N*-methyl-2-pyrrolidone (NMP, Aldrich). The formed slurry was coated on a piece of an aluminum (Al) current collector and dried in a vacuum oven at 120 °C for 12 h. Galvanostatic charge–discharge cycling was performed using a 2032 half-cell, which was assembled with a Li-metal anode and an OLO cathode, a poly(ethylene) (PE) separator, and an electrolyte (EC:EMC=1:2 + 1 M  $\text{LiPF}_6$ ) without additives or with 3% VC, 3% TMSP, or 1.5% VC + 1.5% TMSP, respectively. To examine the half-cell performance, the cells were charged to 4.6 V (vs.  $\text{Li}/\text{Li}^+$ ) and discharged to 2.0 V (vs.  $\text{Li}/\text{Li}^+$ ) repeatedly at a constant current of 0.1 C for two cycles (as a formation step) and followed by 1.0 C for fifty cycles at room temperature using a charge/discharge unit (Toyo, TOSCAT-3100). After the examination of the cycling performances, each cell was dismantled in an Ar-filled glove box, and the resulting electrodes were washed with fresh dimethyl carbonate (DMC). The surface morphologies of each electrode were characterized by field-emission scanning electron microscopy (FE-SEM, Quanta 3D FEG, FEI), and the chemical components were analyzed using a Fourier transform infrared spectrometer (FT-IR, Bruker, VERTEX 70).

## Detailed simulated annealing procedure

After the initial microstructure was generated, minimization of the potential energy of the model was carried out, where the COMPASS force-field was used. Simulated annealing was then performed by raising the temperature from 300 K to 1500 K and then allowing it to cool to 300 K at a rate of 100 K / 5 ps. The conformation was heated again at the same rate in order to jump to a different valley, after which cooling was allowed again. A series of 10 cycles of simulated annealing between 300 and 1500 K was carried out to sample the conformational space effectively. There were 1,200,000 molecular dynamics steps in total for each molecule. The MD simulations were carried out in the microcanonical (NVE) ensemble. The velocity Verlet algorithm with a time step of 1 fs was used for the integration of the atom motion equations throughout all simulations.

The molecular simulations are performed by the Forcite Plus module of the commercial software Materials Studio 5.5 using the COMPASS forcefield. This forcefield enables accurate and simultaneous predictions of structural, conformational, vibrational, and thermophysical properties that exist for organic molecules, inorganic small molecules, and polymers in isolation and in condensed phases, and under a wide range of conditions of temperature and pressure.<sup>7-9</sup>

## References

- 1 K. Xu, *Chem. Rev.*, 2004, **104**, 4303–4417.
- 2 K. Xu, *Chem. Rev.*, 2014, **114**, 11503–11618.
- 3 N.-S. Choi, J.-G. Han, S.-Y. Ha, I. Park and C.-K. Back, *RSC adv.*, 2015, **5**, 2732–2748.
- 4 E. Pretsch, P. Bühlmann and C. Affolter, *Structure Determination of Organic Compounds*, Springer-Verlag, Berlin, 2000.
- 5 P. J. Kocienski, *Protecting Groups*, Georg Thieme Verlag, New York, 2005.
- 6 T. W. Greene and P. G. M. Wuts, *Protective Groups in Organic Synthesis*, J. Wiley & Sons Inc., New York, 1991.

- 7 H. Sun, P. Ren and J. R. Fried, *Theor. Polym. Sci.*, 1998, **8**, 229–246.
- 8 H. Sun, *J. Phys. Chem. B*, 1998, **102**, 7338–7364.
- 9 X. P. Chen, C. A. Yuan, C. K. L. Wong, S. W. Koh and G. Q. Zhang, *Mol. Simul.*, 2011, **37**, 990–996.